Biomatter 2:2, 77–86; April/May/June 2012; © 2012 Landes Bioscience

In vitro degradation and release characteristics of spin coated thin films of PLGA with a "breath figure" morphology

Thiruselvam Ponnusamy,[1] Louise B. Lawson,[2] Lucy C. Freytag,[2] Diane A. Blake,[3] Ramesh S. Ayyala[4] and Vijay T. John[1,*]

[1]Department of Chemical and Biomolecular Engineering; Tulane University; New Orleans, LA USA; [2]Department of Microbiology and Immunology; Tulane University; New Orleans, LA USA; [3]Department of Biochemistry; Tulane University; New Orleans, LA USA; [4]Department of Ophthalmology; Tulane University; New Orleans, LA USA

Keywords: breath figure, PLGA, degradation, drug delivery, microporous thin film

Abbreviations: PLGA, poly (lactic-co-glycolic acid); PEG, poly (ethylene glycol); SEM, scanning electron microscopy

Poly (lactic-co-glycolic acid) (PLGA) coatings on implant materials are widely used in controlled drug delivery applications. Typically, such coatings are made with non-porous films. Here, we have synthesized a thin PLGA film coating with a highly ordered microporous structure using a simple and inexpensive water templating "breath figure" technique. A single stage process combining spin coating and breath figure process was used to obtain drug incorporated porous thin films. The films were characterized by scanning electron microscope (SEM) to observe the surface and bulk features of porosity and also, degradation pattern of the films. Moreover, the effect of addition of small amount of poly (ethylene glycol) (PEG) into PLGA was characterized. SEM analysis revealed an ordered array of ~2 μm sized pores on the surface with the average film thickness measured to be 20 μm. The incorporation of hydrophilic poly (ethylene glycol) (PEG) enhances pore structure uniformity and facilitates ingress of water into the structure. A five week in vitro degradation study showed a gradual deterioration of the breath figure pores. During the course of degradation, the surface pore structure deteriorates to initially flatten the surface. This is followed by the formation of new pinprick pores that eventually grow into a macroporous film prior to film breakup. Salicylic acid (highly water soluble) and Ibuprofen (sparingly water soluble) were chosen as model drug compounds to characterize release rates, which are higher in films of the breath figure morphology rather than in non-porous films. The results are of significance in the design of biodegradable films used as coatings to modulate delivery.

Introduction

Poly (lactic-co-glycolic acid) (PLGA), a biodegradable and biocompatible FDA approved polymer, is being increasingly used in sustained drug delivery applications.[1-6] The polymer undergoes hydrolytic degradation under physiological conditions breaking down into poly (lactic acid) and poly (glycolic acid) and eventually to lactic and glycolic acid, which are easily eliminated by tricarboxylic acid metabolic pathways.[7,8] PLGA coatings on implant materials, such as stents,[3] allow a slow release of drug with the coating eventually being degraded away. Typically, such coatings are made with thin films that are solvent cast on the support material.[3,5,9,10] Such films have very low porosities and after the initial burst of surface bound drug, further release occurs primarily through the degradation of the polymer.[10]

In this paper, we describe the fabrication of very thin films with "breath figure" porous structures of PLGA and correlate the drug delivery characteristics of such films with the details of degradation. Breath figure polymer morphologies were first pioneered by Srinivasarao and coworkers as a simple method to fabricate ordered arrays of pores in a polystyrene film.[11] In this technique, the polymer is dissolved in a low boiling organic solvent and cast under humid conditions resulting in the formation of an ordered pore structure on the film surface[12-15] with a dense under layer. Briefly, the mechanism of pore formation involves the rapid evaporation of the solvent that causes a cooling effect on the polymer solution surface. The cooling induces the condensation of water droplets (from humid air) onto the solution surface. Micron-sized water droplets nucleate on the surface and subsequently grow to form the arrays of "islands" that eventually produces the breath figure pattern. These arrays do not coalesce, but penetrate into the polymer solution, which acts as a substrate for subsequent condensation and nucleation of water droplets. The polymer film forms around water droplet/solution interface and encapsulates the water droplets preventing coalescence. Locally acting lateral capillary forces and convective motion resulting from temperature gradients on the solution surface stabilize the water droplets arranging them in an ordered

*Correspondence to: Vijay T. John; Email: vj@tulane.edu
Submitted: 12/09/11; Revised: 03/14/12; Accepted: 04/16/12
http://dx.doi.org/10.4161/biom.20390

manner.[16,17] Once the film is dried at room temperature, the evaporation of residual solvent and water leads to the formation of a surface patterned with a microporous structure. The breath figure process is simple, economically viable and easily reproducible.[18-22]

Because of the highly porous nature of breath figures, it is possible that release characteristics of encapsulated pharmaceutical compounds can be significantly modified in comparison to non-porous films of the same material. It is therefore important to characterize such release, especially in connection with the fact that the polymer film degrades with time. This paper describes the synthesis of drug-loaded porous PLGA films prepared using the breath figure method and attempts to correlate the release kinetics to the degradation characteristics. A single stage process combining spin coating and the breath figure technique was used to obtain drug incorporated porous thin films. In addition to PLGA, PEG was used as a plasticizer to modify pore structures and release characteristics through incorporation of a hydrophilic polymer into the film. Salicylic acid and Ibuprofen were used as model drugs compounds. Salicylic acid is a water soluble compound (solubility $>$ 2 mg/ml) while ibuprofen has a limited solubility in water (solubility $<$ 0.5 mg/ml). Pioneering work by Wang and coworkers have shown morphological progressions in the degradation of relatively thick nonporous biodegradable films with correlation to the lag phase in drug release.[23] However, the work described in the current paper is the first instance of correlating time-dependent breath figure morphology changes to release characteristics. Potential applications of this study include the design of very thin coatings on medical devices and surgical implants where release profiles can be designed through control of surface structures and/or sandwich type layers.

Results and Discussion

Characterization of "breath figure" patterned thin polymer films. Figure 1A and B show morphological details of breath figure PLGA films in comparison to the nonporous films obtained by spin coating in a dry atmosphere (shown as corresponding insets to the figures). The SEM micrograph in **Figure 1A** reveals an ordered array of approximately 2 μm sized pores on the surface, observed over a large surface area. The pores' dimensions created from PLGA are reproducible and simple to create. **Figure 1B** is an oblique view of the cross section and the surface and reveals both surface features and aspects of bulk porosity. Clearly, the pore structure is prevalent almost throughout the film but ends in a dense bottom layer of around 2 μm thickness. The average thickness of the film measured by a micrometer is 20 μm. The insets to **Figure 1A and B** reveal corresponding morphologies of a spin coated PLGA film without incorporating the breath figure technique. As observed, the film clearly lacks the surface and bulk porosity characteristics of breath figures. **Figure 2A and B** reveal higher magnification top and oblique view images of the PLGA breath figure film. After peeling off the film from the teflon substrate, the dense bottom layer was imaged showing the lack of any discernible pores (inset to **Fig. 2B**).

We have used the analysis described by Bolognesi and co-workers[24] to understand pore penetration in the bulk polymer

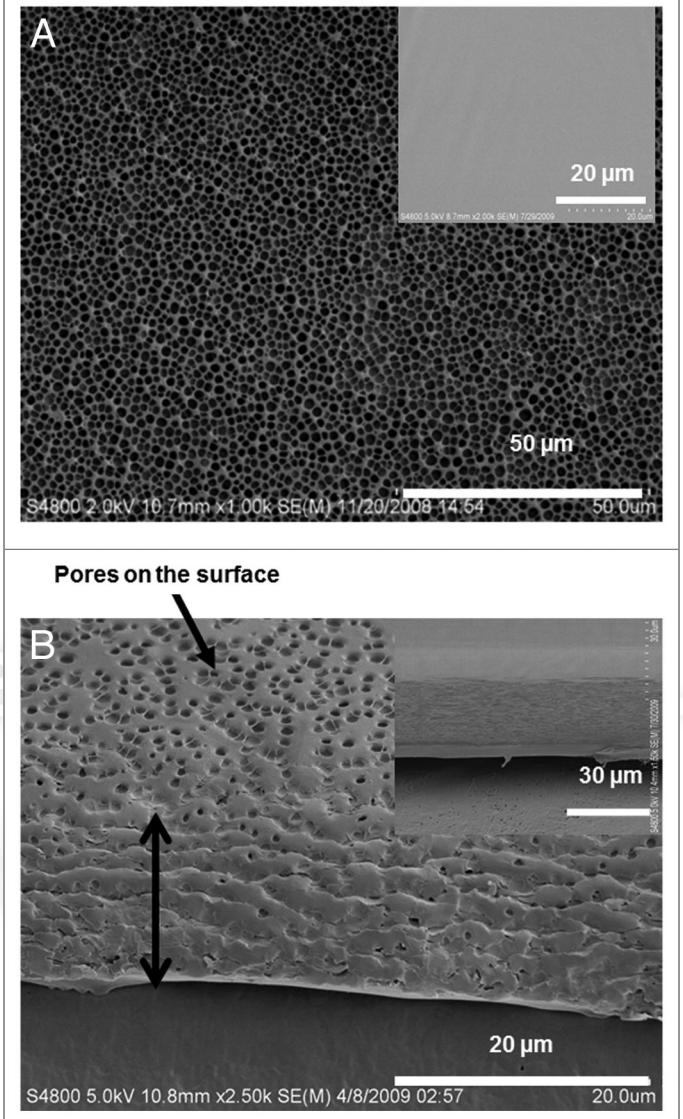

Figure 1. Scanning electron microscopy (SEM) of breath figure PLGA film. (A) Low magnification of surface topography (inset, surface morphology of non-porous PLGA film). (B) Low magnification of cross-sectional view (inset, cross-sectional morphology of non-porous PLGA film).

film. As these authors have stated, pore formation can be described through the minimization of the free energy at the three phase (water droplet, air and polymer solution) interface, with a dimensionless pore penetration $Z_0 = Z/R$ where Z is the distance of the droplet center from the air-solvent interface and R is the droplet radius. Z_0, the value of Z at which the free energy is minimized is expressed as

$$Z_0 = \frac{\gamma_w - \gamma_{w/s}}{\gamma_s} \quad (1)$$

where γ_w and γ_s are the surface tensions of the air-water interface and the air-solvent interface, respectively, and $\gamma_{w/s}$ is the interfacial tension between water and the solvent. For values $-1 < Z_0 < 1$,

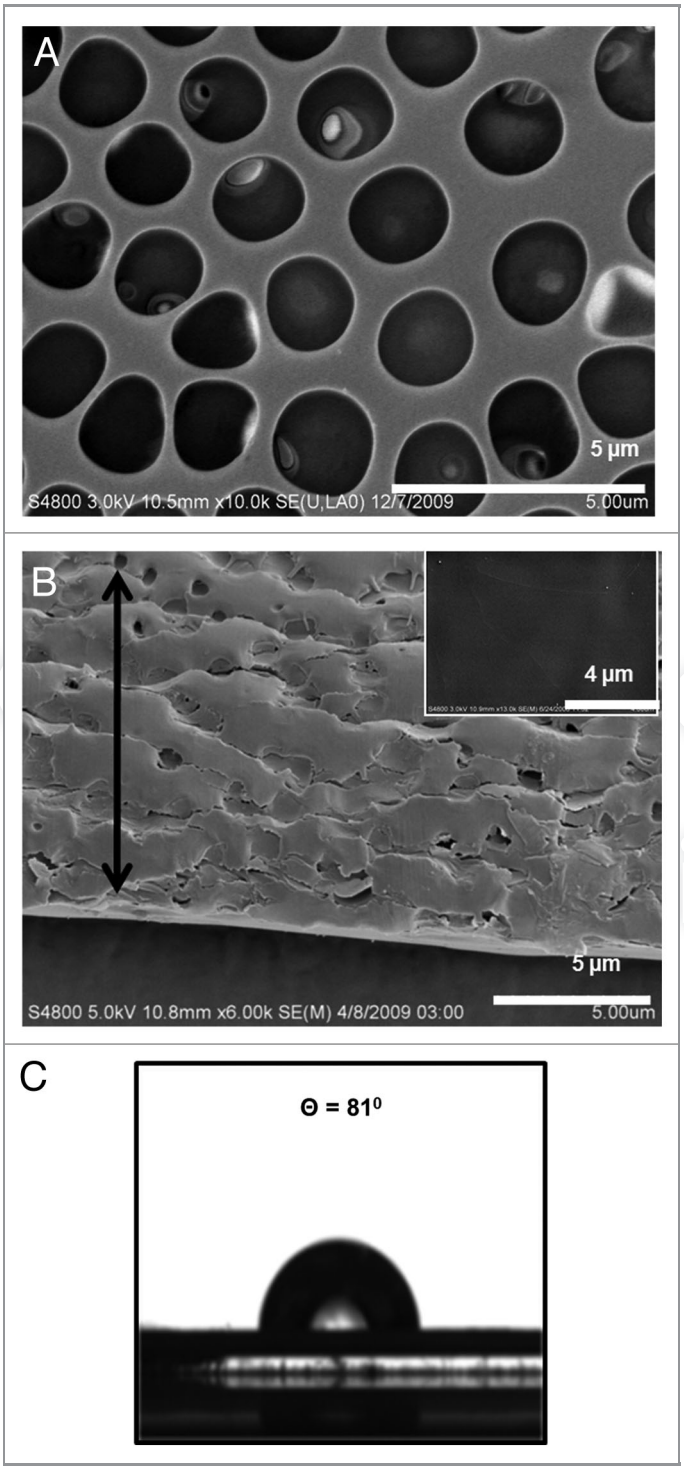

Figure 2. High magnification SEM images of breath figure PLGA film. (A) Surface morphology. (B) Cross-sectional morphology (inset, surface morphology of dense bottom layer). (C) Contact angle of breath figure PLGA film.

the water droplets will be located at the interface between air and solution with partial exposure to both fluids. Upon formation of the final breath figure morphology, such systems will only consist of a single layer of pores below which is a dense nonporous layer.[24]

For Z_0 values greater than unity, the droplets will penetrate below the surface, the consequence of which is a multi-layered porous polymer structure. For the PLGA-methylene chloride system, Z_0 is 1.62, based on the air-water surface tension, γ_w (72.8 dynes/cm), the air-methylene chloride surface tension, γ_s (28.12 dynes/cm) and the water-methylene chloride interfacial tension, $\gamma_{w/s}$ (27.2 dynes/cm).[25] The deep penetration of pores in the PLGA system studied here is due to the penetration of water droplets below the solvent-air interface. **Figure 2C** shows the droplet shape for contact angle determination of breath figure PLGA, from which a value of 81° was obtained, indicating the relative hydrophobicity of the material.

Poly (ethylene glycol) (PEG) is a well-studied plasticizer for PLGA and as a hydrophilic material is expected to increase hydrophilicity of breath figure films.[23] We have found that PEG incorporation leads to a much better definition of pore structure and an enhanced hydrophilicity. **Figure 3** illustrates the influence of PEG addition at a 1:9 ratio of PEG to PLGA. The pore structure is highly monodisperse with the pores arranged in ordered hexagonal arrays, as shown in **Figure 3A and B.** The addition of small quantity of PEG improves the degree of ordering and orientation of pores. Again, we see the deep penetration of pores into the polymer film (**Fig. 3C**) with an almost row-by-row arrangement. Our experiments indicate that the optimal PEG incorporation level is approximately 10 wt% and when PEG is added to values greater than 15 wt %, the film tends to become patchy (data not shown for brevity). **Figure 3D** indicates that the PEG incorporated breath figure has enhanced hydrophilicity as shown by a contact angle of 67°. Imaging software (Image-Pro Plus version 5.0) was used to measure pore size distributions. A minimum of three SEM images were used with the dimensions of 200 pores measured to obtain statistics on pore size distributions. The average pore diameters are 1.4 µm and 2.5 µm for the breath figure PLGA and PEG/PLGA films, respectively and the corresponding standard deviations are 0.296 µm and 0.668 µm.

The incorporation of breath figure morphologies significantly adds to surface areas of the film. For example, if the surface pores are assumed to be hemispheres, the surface area occupied by each pore ($2\pi r^2$) is double that of the equivalent flat surface (πr^2). Assuming hexagonal order in the surface pores, with a pore to pore distance "a" (center to center distance of 2r + a), it is derived that the fractional increase in surface area per unit cell on the film surface is $[\pi r^2/(2r + a)^2\cos(\pi/6)]$ which translates into an increase of 58% with pores of radius, r = 1 µm and pore to pore distances, a = 0.5 µm as example dimensions. With the deep penetration of pores into the breath figure films, it is expected that release rates would be further enhanced as the polymer gradually degrades exposing underlying pores.

In vitro degradation of breath figure films. *Degradation of PLGA films.* **Figure 4** illustrates the morphological characteristics of the degradation of the breath figure film over a period of 35 days. To simulate an environment where the film is used as a coating for medical devices, we examined films coated on a teflon substrate so that the degradation is primarily through the porous breath figure surface. Within seven days, clear morphological changes are observed with the deterioration of the top layer of

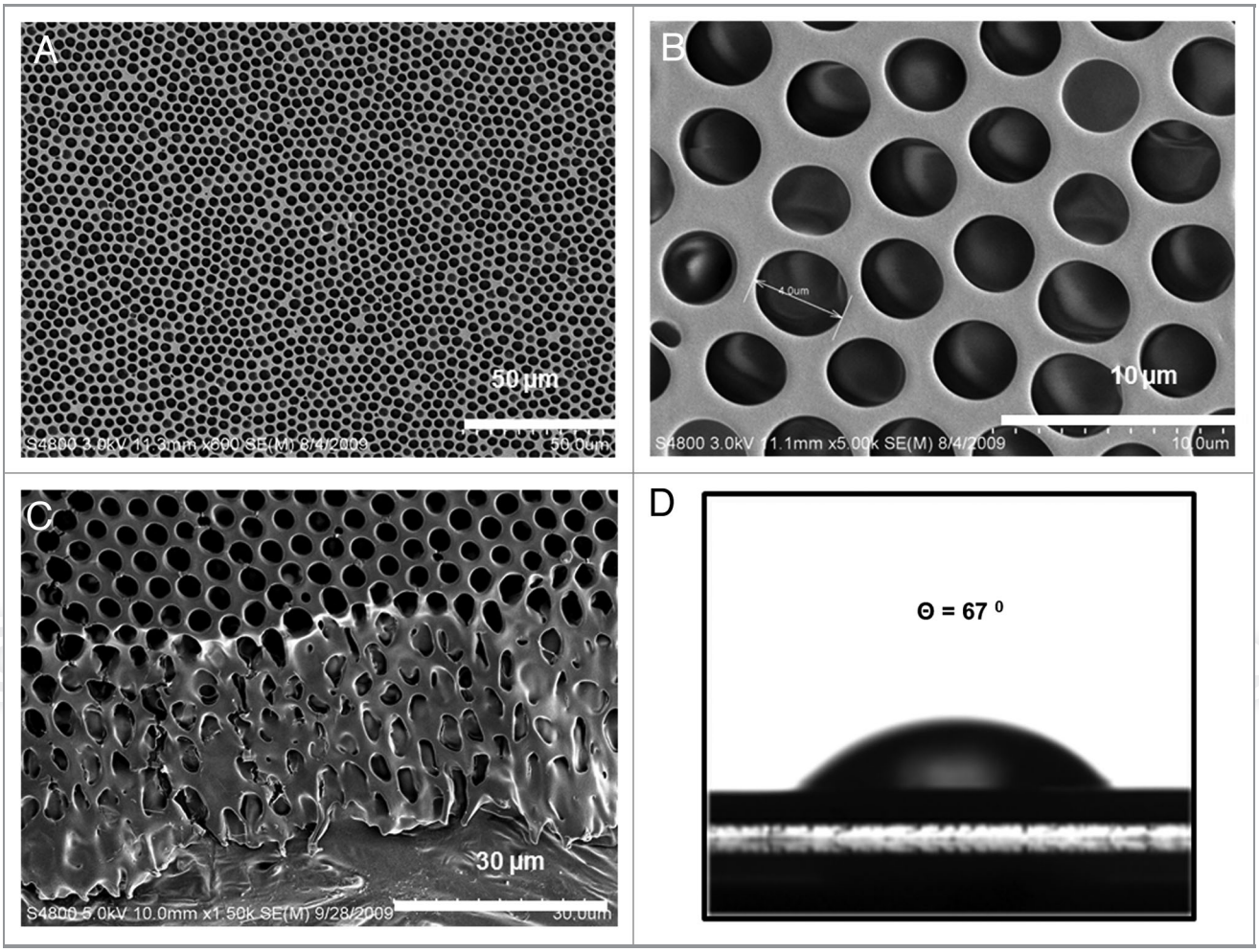

Figure 3. SEM of breath figure PEG/PLGA film. Low (A) and high (B) magnification of surface morphology. (C) Cross-sectional morphology. (D) Contact angle of breath figure PEG/PLGA film.

pore walls leading to a flatter topology as shown by the arrow in **Figure 4A** (day 7). As degradation proceeds, intervening ridges between the pores become less distinct as the surface layers are degraded. The surface pores eventually become depressions on the surface of the film as the ridges dissolve away. The side view (**Fig. 4B**, day 7) also illustrates that the film has significantly decreased in thickness to 5–10 µm. With time the pores in the lower layers of the original film become revealed as the polymer surface continues to degrade (box in **Fig. 4A**, day 14). We note however that as degradation proceeds to the vicinity of the originally dense non porous bottom layer, small submicron pinprick pores are generated that are not part of the original breath figure structure. The pinprick pores are denoted by the arrows in the micrographs denoting day 21 degradation characteristics. The number density of these pinprick pores increases (after 28 days) and the film begins to break up. In 35 days, cracks and islands of macroporous film remnants are observed. The surface of the film also becomes wrinkled. We find that throughout the degradation process, the film continues to adhere to the teflon substrate.

Degradation of PEG/PLGA films. **Figure 5A and B** show the effect of PEG in the degradation of PLGA film. Essentially the same progression of deterioration is observed with an initial surface flattening, the exposure of underlying pores, and the eventual formation of new pinprick pores that grow and eventually rupture the film. The addition of PEG may increase the degradation rate as we observe the initial morphological change of underlying pores coming into view is apparent within seven days of degradation.

These observations are useful as the sequence of events that lead to film breakup through degradation is not evident. It is interesting that the initial pores of the breath figure do not propagate into larger pores leading to rupture. Rather, there is an initial flattening of surface topography and then the emergence of new underlying pores.

Release characteristics of breath figure polymer films. The release profile of breath figure PLGA and PEG/PLGA films was performed in PBS medium (pH 7.4, 0.1M), incubated at 37°C. A non-porous film with the equivalent amount of dispersed drug was used as control. The choice of salicylic acid as a model

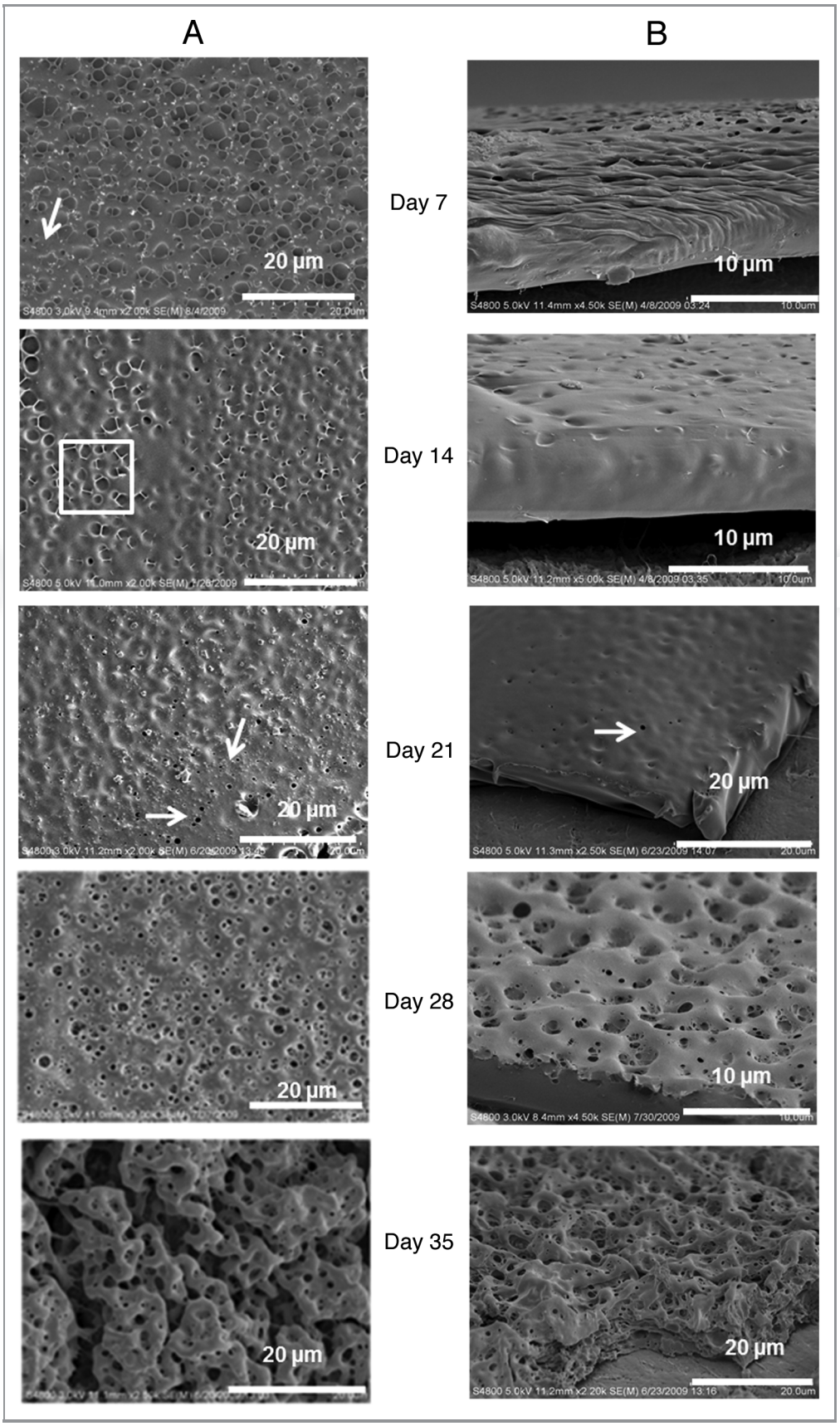

Figure 4. In vitro degradation pattern of breath figure PLGA film for 35 d. (A) Surface morphology. (B) Cross-sectional morphology.

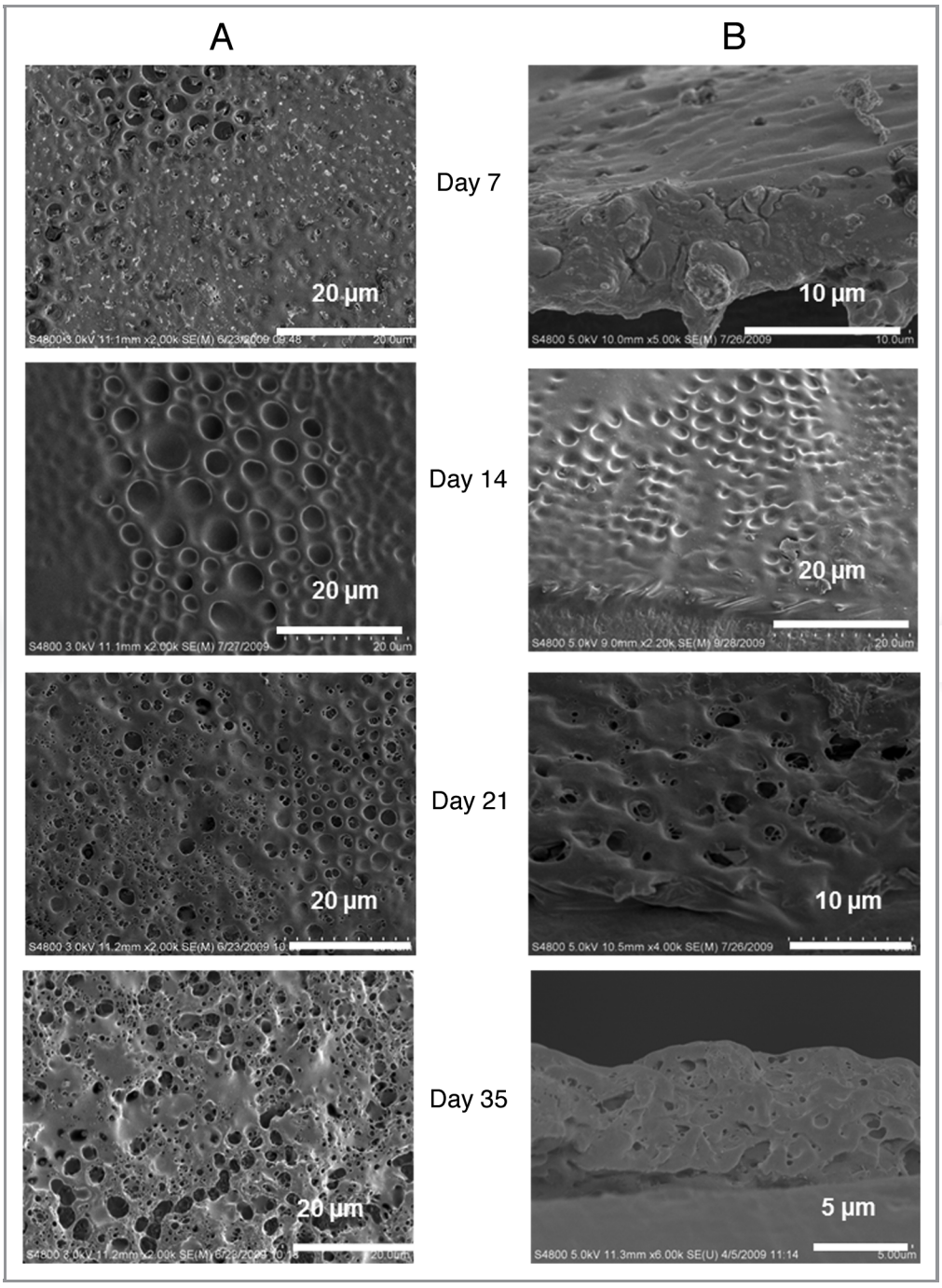

Figure 5. In vitro degradation pattern of breath figure PEG/PLGA film for 35 d. (A) Surface morphology. (B) Cross-sectional morphology.

drug component is due to its high water solubility (> 2 mg/mL) and clearly measurable UV absorbance at 296 nm. **Figure 6A** illustrates the cumulative release of salicylic acid from the PLGA film and PEG/PLGA film respectively, for a period of eight days. The release illustrates the effects of breath figure morphology and the role of incorporating PEG into the film. We note that within 3 h, differences between the breath figures and the corresponding non-porous films, and between PLGA and PEG/PLGA films are observed, and the differences become more pronounced at later times. All films with the breath figure morphology show a higher release rate than the corresponding non-breath figure, and the PEG/PLGA films show increased release rates compared with direct PLGA films. We also note that most of the release is completed within five days during which there are changes in surface topography, but no formation of pinprick pores and breakdown of the film.

The situation is similar in the case of ibuprofen (**Fig. 6B**) although release takes place over a longer period which involves

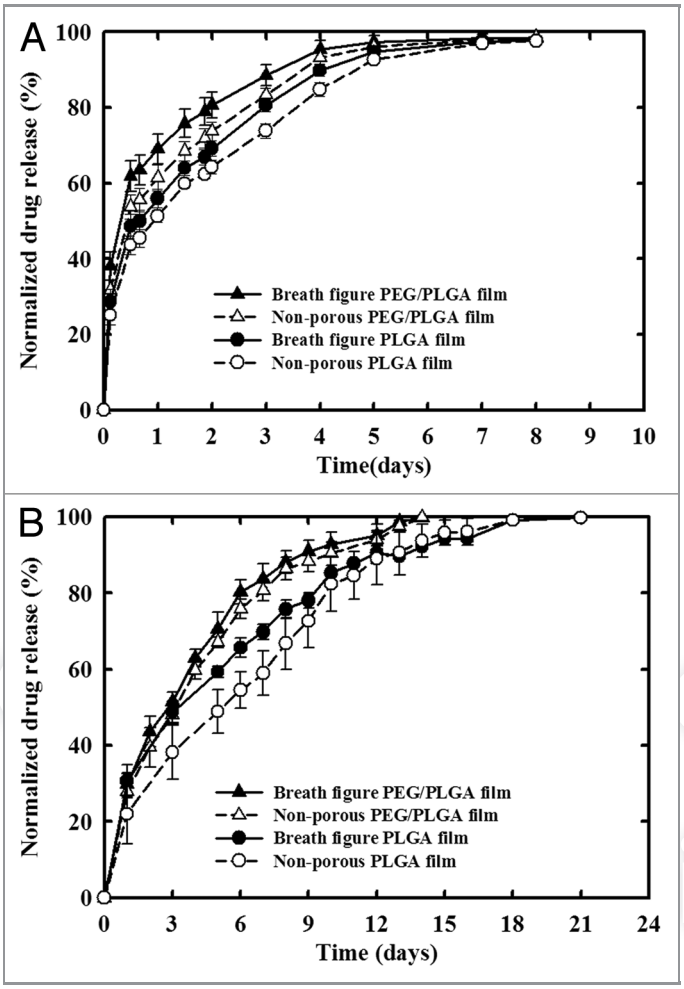

Figure 6. In vitro release characteristics of breath figure and non-porous polymer films. (A) Release profile of Salicylic acid from PLGA and PEG/PLGA films. (B) Release profile of Ibuprofen from PLGA and PEG/PLGA films.

the formation of pinprick pores during the latter release stages and the gradual initiation of film breakdown. Again, breath figure morphologies indicate faster release than the corresponding non-porous analogs. However, we do see that the incorporation of PEG in the nonporous film enhances release over the pure PLGA breath figure indicating the strong role played by PEG in allowing water ingress.

In thin films where release is through Fickian diffusion, M_t/M_∞ the fractional release can be expressed as[23,26]

$$\frac{M_t}{M_0} = 4\left(\frac{Dt}{\pi l^2}\right)^{\frac{1}{2}} = kt^{\frac{1}{2}} \quad (2)$$

the traditional formulation for transient diffusion in a slab at small values of the dimensionless time $\left(\frac{Dt}{\pi l^2}\right)$, where D is the diffusivity, l is the slab thickness and k a lumped parameter.[26] In situations when release is entirely through dissolution of the polymer matrix, the release rate is independent of time, therefore leading to

$$\frac{M_t}{M_0} = k't \,. \quad (3)$$

One can therefore write a heuristic expression

$$\frac{M_t}{M_0} = k^* t^n \quad (4)$$

where n values close to 0.5 indicate diffusion as the primary release mechanism while n values close to unity indicate degradation as driving release. Values of k* and n are listed in **Table 1** for both systems. The significant deviation from the exponent of unity in the correlation for both salicylic acid and ibuprofen release implies that transport through diffusion dominates over release due to the degradation of the polymer. With such thin films, we do not see an extended lag phase that would indicate the secondary phase where degradation becomes the primary driver for release. Even with the formation of pinprick pores initiating the film degradation process during the release period for ibuprofen, thin films of such materials allow encapsulated species to diffuse relatively small distances to the film surface for release with diffusion being the primary mode of release.

Materials and Methods

Poly (D,L-lactide-co-glycolide) (PLGA 50:50) polymer (Resomer RG 504 M_w = 56,000 and inherent viscosity = 0.56 dl/g) was purchased from Boehringer Ingelheim Chemicals Inc. Methylene chloride (organic solvent, ACS grade) was obtained from Fisher Scientific. Teflon sheets, 0.2 mm thick, used as substrate materials, were purchased from Scientific Commodities Inc. (BB9558). All other chemicals, Poly (ethylene glycol)(PEG-Average M_w = 3350 g/mol, P3640), Ibuprofen (≥ 98% GC, I4883), salicylic acid (99%, S9763), disodium hydrogen phosphate (Na_2HPO_4), potassium dihydrogen phosphate (KH_2PO_4), sodium chloride (NaCl) and potassium chloride (KCl) were obtained from Sigma Aldrich Chemicals. All chemicals were used as received, without further purification.

Synthesis of "breath figure" PLGA polymer films. A spin coater (model WS-400-6NPP-LITE, Laurell Technologies Corporation) was used to prepare the film. A 1.5 cm square piece of teflon, used as the substrate was rinsed with 95% ethanol to remove any surface contaminants. The substrate was then placed on the spin table which is connected to a vacuum to hold the

Table 1. Values of the exponent n and rate constant k* for all polymer films

Polymer films	Salicylic acid			Ibuprofen		
	n	k*	R^2	n	k*	R^2
Breath figure PLGA	0.32	0.78	0.99	0.43	0.60	0.99
Non-porous PLGA	0.34	0.75	0.99	0.57	0.51	0.99
Breath figure PEG/PLGA	0.25	0.85	0.98	0.51	0.60	0.99
Non-porous PEG/PLGA	0.29	0.81	0.99	0.54	0.57	0.99

R^2 is the regression coefficient.

substrate while spinning. The coating chamber is connected to a flow of humid air created by bubbling the air through the distilled water. Although the humidity can be modified by mixing the air with dry nitrogen, in our experiments, we maintained the relative humidity at about 70% as measured by a hygrometer (Fisher Scientific).

Figure 7 illustrates the entire process of breath figure thin film fabrication. To prepare the coating solution, 1% (w/v) of the drug (ibuprofen or salicylic acid) was first dissolved in methylene chloride followed by dissolving 15% (w/v) of the PLGA polymer. The solution was vortex mixed to ensure homogeneity. The appropriate volume (0.4 mL) of the solution containing PLGA and the drug (67 µg drug/mg polymer) was dropped onto the substrate and the spinning process was immediately accelerated to 2,500 rpm for 30 sec. During the spin coating process, the solvent evaporates to form an opaque film. The coated films were dried for at least a day at room temperature. In experiments with PEG, the ratio of PEG to PLGA was 1:9. Similar procedures were followed to prepare control breath figure films without the drug component. To prepare non-porous films, the gas supply was switched from humid air to dry nitrogen. All films were easily peeled off from the teflon substrate. To clearly obtain release and morphological characteristics from breath figure coated systems, the films were reattached to teflon squares using double-sided tape (3M). This ensures that both release and degradation will occur primarily from the porous surface of the film. Verification of drug content in the polymer film was done by redissolving the thin polymer film in an excess of dichloromethane, removing the solvent (to create very small particles of the polymer) to precipitate the drug and then extracting the drug into phosphate buffered saline solution (PBS) for analysis.

Characterization and analysis of breath figure polymer film. *Film morphology.* Morphological characterizations of all films were done using a field emission scanning electron microscopy (FE-SEM; Hitachi S-4800) at an accelerating voltage of 3 kV. The films were mounted on the SEM sample holder and gold coated using a sputter coater (Polaron SEM coating system) set at 20 mA for duration of 75 sec. All films were imaged in the dry state which is appropriate for PLGA films which in contrast to hydrogels, do not absorb water significantly and therefore do not change morphology. A minimum of three films were examined to characterize surface and bulk morphologies.

In vitro degradation of breath figure polymer film. Experiments to understand the in vitro degradation of breath figure PLGA and PEG/PLGA films were done at 37°C in phosphate buffered saline solution (PBS) (137 mM NaCl, 2.7 mM KCl, 10 mM Sodium Phosphate dibasic and 2 mM Potassium Phosphate monobasic). The pH was then adjusted to 7.4 using 0.1M HCl. The films coated on teflon were suspended and incubated in the buffer solution for 35 d, and subjected to slow stirring using a magnetic stir bar. The PBS medium was changed every week to maintain constant pH. Each week, a small piece of polymer film was cut from the original film, rinsed carefully with distilled water and dried at room temperature for at least a day prior to imaging. The experiments were conducted in triplicate.

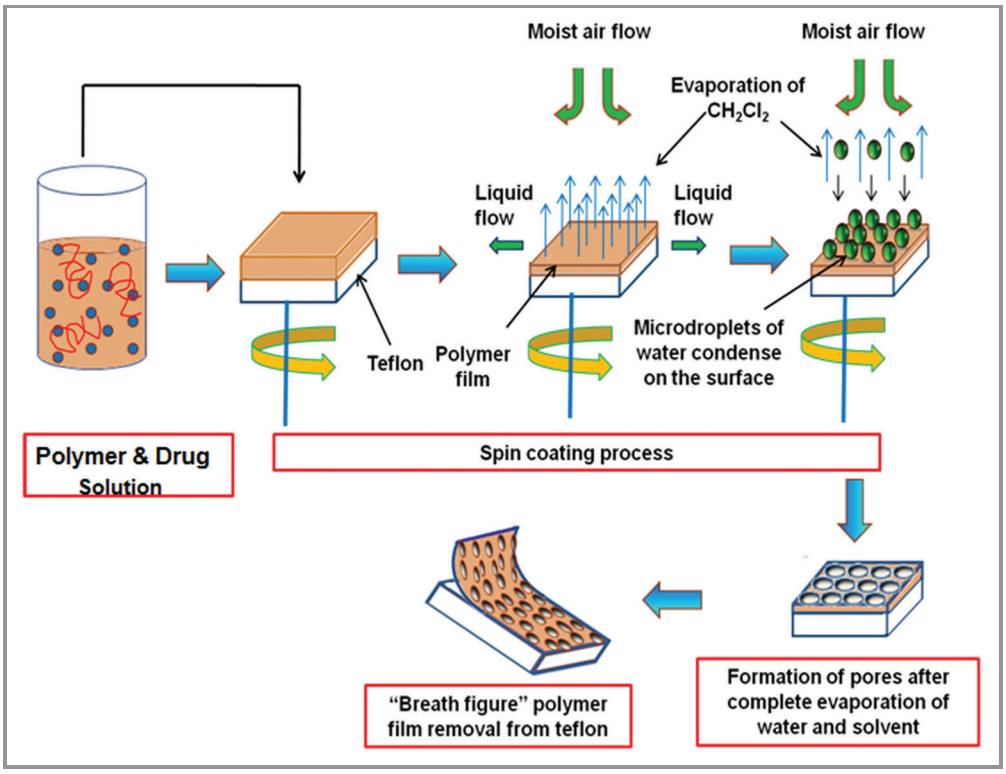

Figure 7. Mechanism of drug incorporation into thin PLGA film using the breath figure and spin coating technique.

Surface contact angle measurements. The wettability of breath figure films was measured using the sessile drop method with a standard goniometer (Rame-Hart model 250) and analyzed using the DROPimage Advanced software for contact angle determination. A 3 μL distilled water droplet was placed on the polymer film surface and the contact angle 'θ' measured. The measurement was done for a minimum of five samples of a specific polymer film, and the average value reported. Typical standard deviations are of the order of 0.3.

In vitro release characteristics. Ibuprofen and Salicylic acid were used as model drugs to characterize the release profiles of breath figure polymer films. The equivalent non-porous smooth films were used as controls. In vitro release studies were performed by incubating 1.5 cm side square drug incorporated films in 15 ml of PBS medium at 37°C and stirred gently using a magnetic stirrer. At specific time intervals, 0.650 ml aliquots of the solution was withdrawn and centrifuged to remove any possible debris from the degrading polymer. Then, the aliquot was returned to the vial after measuring the absorbance to quantify drug release. The pH of the medium was monitored during the course of the experiment to verify that the solution is buffered adequately during polymer degradation. Ibuprofen and salicylic acid release were quantified through the absorbance at 221 and 296 nm, respectively. Standard calibration plots of ibuprofen and salicylic acid absorbance were constructed to correlate absorbance with drug release levels. All experiments were conducted in triplicate.

Conclusions

Morphological characteristics of breath figure films of degradable PLGA and PEG/PLGA materials were analyzed through scanning electron microscopy as they were allowed to degrade in vitro. The degradation pattern shows a flattening of surface structure where the walls of the surface breath figure pores are first degraded away, followed by the gradual degradation of the underlying layers. Pinprick pores extending to the base of the film are subsequently formed which evolve into larger pore structures that eventually break up the film.

The morphology of the film has a significant effect on release characteristics with breath figure morphologies in general exhibiting faster release than their nonporous analogs. Additionally the incorporation of poly (ethylene glycol) into the films enhances release rates, which we attribute to improvement of water ingress into the film. Drug release from such thin films appears to follow diffusion pathways rather than a constant release rate based on degradation of the material through dissolution of surface layers.

The use of breath figure morphologies in biodegradable polymer films adds an additional level of control to drug release. Coating medical devices (stents, surgical meshes, etc.) with thin biodegradable films allows exploitation of controlled release without significant modifications of the mechanical properties of the substrate materials. For example, coated surgical meshes need to retain the highly flexible nature of the underlying synthetic or tissue-based material. The detailed applications of breath figure films to in vivo applications will be detailed in subsequent publications.

Disclosure of Potential Conflicts of Interest

No potential conflicts of interest were disclosed.

Acknowledgments

This work was supported by the Louisiana Board of Regents. Additional support from the US Army Medical Research and Material Command under Award W81XWH-10-1-0377 is gratefully acknowledged.

References

1. Hickey T, Kreutzer D, Burgess DJ, Moussy F. Dexamethasone/PLGA microspheres for continuous delivery of an anti-inflammatory drug for implantable medical devices. Biomaterials 2002; 23:1649-56; PMID:11922468; http://dx.doi.org/10.1016/S0142-9612(01)00291-5
2. Ramgopal Y, Venkatraman SS, Godbey WT. In vitro release of complexed pDNA from biodegradable polymer films. J Appl Polym Sci 2008; 108:659-64; http://dx.doi.org/10.1002/app.27672
3. Westedt U, Wittmar M, Hellwig M, Hanefeld P, Greiner A, Schaper AK, et al. Paclitaxel releasing films consisting of poly(vinyl alcohol)-graft-poly(lactide-co-glycolide) and their potential as biodegradable stent coatings. J Control Release 2006; 111:235-46; PMID:16466824; http://dx.doi.org/10.1016/j.jconrel.2005.12.012
4. Xu Q, Czernuszka JT. Controlled release of amoxicillin from hydroxyapatite-coated poly(lactic-co-glycolic acid) microspheres. J Control Release 2008; 127:146-53; PMID:18325617; http://dx.doi.org/10.1016/j.jconrel.2008.01.017
5. Dorta MJ, Santoveña A, Llabrés M, Fariña JB. Potential applications of PLGA film-implants in modulating in vitro drugs release. Int J Pharm 2002; 248:149-56; PMID:12429469; http://dx.doi.org/10.1016/S0378-5173(02)00431-3
6. Ramchandani M, Robinson D. In vitro and in vivo release of ciprofloxacin from PLGA 50:50 implants. J Control Release 1998; 54:167-75; PMID:9724903; http://dx.doi.org/10.1016/S0168-3659(97)00113-2
7. Göpferich A. Mechanisms of polymer degradation and erosion. Biomaterials 1996; 17:103-14; PMID:8624387; http://dx.doi.org/10.1016/0142-9612(96)85755-3
8. Alexis F. Factors affecting the degradation and drug-release mechanism of poly(lactic acid) and poly. [(lactic acid)-co-(glycolic acid)]. Polym Int 2005; 54:36-46; http://dx.doi.org/10.1002/pi.1697
9. Lao LL, Venkatraman SS, Peppas NA. Modeling of drug release from biodegradable polymer blends. Eur J Pharm Biopharm 2008; 70:796-803; PMID:18577449; http://dx.doi.org/10.1016/j.ejpb.2008.05.024
10. Chiu LK, Chiu WJ, Cheng YL. Effects of polymer degradation on drug release a mechanistic study of morphology and transport properties in 50:50 poly(dl-lactide-co-glycolide). Int J Pharm 1995; 126:169-78; http://dx.doi.org/10.1016/0378-5173(95)04119-2
11. Srinivasarao M, Collings D, Philips A, Patel S. Three-dimensionally ordered array of air bubbles in a polymer film. Science 2001; 292:79-83; PMID:11292866; http://dx.doi.org/10.1126/science.1057887
12. Madej W, Budkowski A, Raczkowska J, Rysz J. Breath figures in polymer and polymer blend films spin-coated in dry and humid ambience. Langmuir 2008; 24:3517-24; PMID:18294016; http://dx.doi.org/10.1021/la703363a
13. Park MS, Kim JK. Breath figure patterns prepared by spin coating in a dry environment. Langmuir 2004; 20:5347-52; PMID:15986672; http://dx.doi.org/10.1021/la035915g
14. Wong KH, Hernandez-Guerrero M, Granville AM, Davis TP, Barner-Kowollik C, Stenzel MH. Water-assisted formation of honeycomb structured porous films. J Porous Mater 2006; 13:213-23; http://dx.doi.org/10.1007/s10934-006-8007-4
15. Stenzel MH, Barner-Kowollik C, Davis TP. Formation of honeycomb-structured, porous films via breath figures with different polymer architectures. J Polym Sci Pol Chem 2006; 44:2363-75; http://dx.doi.org/10.1002/pola.21334
16. Dell'Aversana P, Neitzel GP. When liquids stay dry. Phys Today 1998; 51:38-41; http://dx.doi.org/10.1063/1.882133

17. Stenzel MH. Formation of regular honeycomb-patterned porous film by self-organization. Aust J Chem 2002; 55:239-43; http://dx.doi.org/10.1071/CH02056
18. Park JS, Lee SH, Han TH, Kim SO. Hierarchically ordered polymer films by templated organization of aqueous droplets. Adv Funct Mater 2007; 17:2315-20; http://dx.doi.org/10.1002/adfm.200601141
19. Zhao BH, Zhang J, Wang XD, Li CX. Water-assisted fabrication of honeycomb structure porous film from poly(L-lactide). J Mater Chem 2006; 16:509-13; http://dx.doi.org/10.1039/b512398d
20. Saunders AE, Dickson JL, Shah PS, Lee MY, Lim KT, Johnston KP, et al. Breath figure templated self-assembly of porous diblock copolymer films. Phys Rev E Stat Nonlin Soft Matter Phys 2006; 73:031608; PMID: 16605538; http://dx.doi.org/10.1103/PhysRevE.73.031608
21. Tian Y, Ding HY, Shi YQ, Jiao QZ, Wang XL. Water-assisted formation of honeycomb films of poly(L-lactic-co-glycolic acid). J Appl Polym Sci 2006; 100:1013-8; http://dx.doi.org/10.1002/app.22926
22. Wu XJ, Jones MD, Davidson MG, Chaudhuri JB, Ellis MJ. Surfactant-free poly(lactide-co-glycolide) honeycomb films for tissue engineering: relating solvent, monomer ratio and humidity to scaffold structure. Biotechnol Lett 2011; 33:423-30; PMID:20960219; http://dx.doi.org/10.1007/s10529-010-0438-y
23. Wang X, Venkatraman SS, Boey FY, Loo JS, Tan LP. Controlled release of sirolimus from a multilayered PLGA stent matrix. Biomaterials 2006; 27:5588-95; PMID:16879865; http://dx.doi.org/10.1016/j.biomaterials.2006.07.016
24. Bolognesi A, Mercogliano C, Yunus S, Civardi M, Comoretto D, Turturro A. Self-organization of polystyrenes into ordered microstructured films and their replication by soft lithography. Langmuir 2005; 21:3480-5; PMID:15807591; http://dx.doi.org/10.1021/la047427u
25. Saien J, Akbari S. Variations of interfacial tension of the n-butyl acetate plus water system with sodium dodecyl sulfate from (15 to 22) degrees C and pH between 6 and 9. J Chem Eng Data 2008; 53:525-30; http://dx.doi.org/10.1021/je700622n
26. Ritger PL, Peppas NA. A simple equation for description of solute release II. Fickian and anomalous release from swellable devices. J Control Release 1987; 5:37-42; http://dx.doi.org/10.1016/0168-3659(87)90035-6